Rev. Int. Contam. Ambie. 42, 79-92, 2026
https://doi.org/10.20937/RICA.55606

DEVELOPMENT AND CHARACTERIZATION OF ACTIVATED CARBON FROM PINE SAWDUST WASTE FOR REMOVAL OF 17-α-ETHINYLESTRADIOL IN A WATER MODEL

Desarrollo y caracterización de carbón activado de residuos de aserrín de pino para la remoción de 17-α-etinilestradiol en un modelo de agua

Karen Nallely RODRÍGUEZ-GAMIZ, José Antonio ÁVILA-REYES, Laura Silvia GONZÁLEZ-VALDEZ, Rene TORRES-RICARIO, Eli Amanda DELGADO-ALVARADO and Marcela Verónica GUTIÉRREZ VELÁZQUEZ*

Centro Interdisciplinario de Investigación para el Desarrollo Integral Regional, Unidad Durango, Instituto Politécnico Nacional, Sigma 119, 20 de Noviembre II, 34220 Durango, Durango, México.

*Author for correspondence: mvgutierrezv@ipn.mx

(Received: May, 2025; Accepted: October, 2025)

Key words: biosorption, agroforestry residues, emerging contaminants, hormones.

ABSTRACT

Activated carbon biosorption is a feasible alternative for both the removal of emerging contaminants from water and for the utilization of agro-industrial waste. 17-α-ethinylestradiol (EE2) is a hormone considered an emerging contaminant in water bodies, which causes physiological alterations in aquatic animals and ecological problems in aquatic ecosystems. In Mexico, 2.3 million cubic meters of agroforestry waste are generated in the sawmill industry. The primary waste from this industry is sawdust, which is either used as fuel or left in fields, thereby causing pollution. The aim of the current study was to determine the potential of activated carbons made from pine sawdust using inexpensive methods (different H_3PO_4 treatments) for the removal of EE2 in a water model. The biosorbents were characterized by their yield and surface changes using infrared spectroscopy, scanning electron microscopy, energy-dispersive spectroscopy, X-ray diffraction, and specific surface area analysis with the Brunauer-Emmett-Teller (BET) method. To determine the EE2 removal capacity, five concentrations of activated carbon (68, 400, 1200, 2000, and 2331 mg/L) at different pH conditions (1.7, 3, 6, 9 and 10.2), and an EE2 solution (400 mg/L water-ethanol, 7:3 v/v) were used. EE2 quantification was carried out by high-performance liquid chromatography with a photodiode array detector (HPLC-PDA). Three activated carbons were prepared, highlighting specific surface area (from 543 to 571.7 m^2/g). Although there were no significant differences, the highest EE2 removal (26.92%) was obtained with activated carbon 2 (AC2) for a treatment of 2331 mg/L and pH 6. The results revealed that pine sawdust is an adequate material for producing efficiently activated carbon for removing EE2 from water through inexpensive methods.

Palabras clave: biosorción, residuos agroforestales, contaminantes emergentes, hormonas.

RESUMEN

La biosorción con carbón activado es una alternativa viable tanto para la remoción de contaminantes emergentes del agua como para el aprovechamiento de residuos

agroindustriales. El 17-α-etinilestradiol (EE2) es una hormona considerada un contaminante emergente en cuerpos de agua, que puede causar alteraciones fisiológicas en animales acuáticos y problemas ecológicos en ecosistemas acuáticos. En México, 2.3 millones de metros cúbicos de residuos agroforestales se generan en la industria del aserrío. El principal residuo de esta industria es el aserrín, que se usa como combustible o se abandona en el campo, lo que causa contaminación. El objetivo del presente estudio fue determinar el potencial de carbones activados fabricados a partir de aserrín de pino mediante métodos económicos (distintos tratamientos con H_3PO_4) para remover EE2 en un modelo de agua. Los biosorbentes fueron caracterizados por su rendimiento y por sus cambios superficiales mediante espectroscopía infrarroja, microscopía electrónica de barrido, espectroscopia de energía dispersiva, difracción de rayos X y análisis de superficie específica por el método Brunauer-Emmett-Teller (BET). Para determinar la capacidad de remoción de EE2, se utilizaron cinco cantidades de carbón activado (68, 400, 1200, 2000 y 2331 mg/L) a diferentes condiciones de pH (1.7, 3, 6, 9 y 10.2), y una concentración de la solución de EE2 de 400 mg/L (agua-etanol, 7:3 v/v). La cuantificación de EE2 se llevó a cabo en un cromatógrafo de líquidos de alta resolución con detector de arreglo de diodos (HPLC-PDA). Se prepararon tres carbones resaltando su área superficial específica (de 543 a 571.7 m^2/g). Aunque no se observaron diferencias significativas, la mayor remoción de EE2 (26.92 %) se obtuvo con AC2, para el tratamiento de 2331 mg/L y pH 6. Los resultados revelaron que el aserrín de pino es un material adecuado para producir, a través de métodos más económicos, carbón activado eficiente para remover EE2 de agua.

INTRODUCTION

17-α-ethinylestradiol (EE2) is a synthetic estrogenic hormone widely used in both human and veterinary medicine for contraception, hormonal therapy, and cancer treatment (Oropesa 2008, Ramírez-Sánchez et al. 2015, Sirén y El Fellah 2017). It is considered an emerging contaminant, commonly detected in water (Oropesa et al. 2017). EE2 has been detected in aquatic systems at trace levels (from 0.05 ng/L to 0.8 mg/L); however, its presence in these systems has brought an increase of concern due to endocrine disruption, alteration of reproductive organs, liver and kidneys, and feminization of aquatic organisms (Gogoi et al. 2018, Ali et al. 2024). All these effects can, in the long term, lead to negative consequences for populations of exposed species (Oropesa et al. 2017).

Hormone removal is not optimal by primary and secondary treatments included in wastewater treatment plants (WWTP), where removal percentages of approximately 6% have been reported for hormone concentrations of 1 µg/L (Bundy et al. 2007). This is why various methods have been developed, including membrane processes and advanced oxidation processes. However, these methods are expensive, their implementation and maintenance are complicated, and they can generate toxic compounds (Sophia and Lima 2018). Another option with global applicability is adsorption using activated carbon (Gogoi et al. 2018, Richardson and Ternes 2018, Osman et al. 2023). This method has several advantages, such as its potential to develop a high contact surface, its high thermostability and efficiency, its simple design and management, and its low cost (Rovani et al. 2014, Sophia and Lima 2018, Cabrera et al. 2020, Osman et al. 2023).

In addition, the preparation of activated carbon from agroforestry residues represents an alternative for waste management, contributing to pollutant reduction in the environment and adding value to waste (Rovani et al. 2014, Pimentel et al. 2024). Activated carbon can remove dyes, metals, methane, and carbon dioxide (Vidal et al. 2018). Activated carbon made from pine sawdust has primarily been used as an adsorbent to remove basic contaminants such as dyes and metals (Arévalo and Reátegui 2020). However, information about the removal of emerging contaminants, especially hormones, is scarce (Rovani et al. 2014, 2016).

Textural, morphological, and chemical properties of activated carbon are variable according to the material from which it is prepared and also the physical and chemical conditions of preparation (Álvarez-Torrellas et al. 2016). This makes it necessary to evaluate these parameters to obtain efficient activated carbons.

The genus *Pinus* (Pinaceae) represents 70.5% of timber production in Mexico, generating 2.3 million cubic meters of agroforestry waste/year (Fregoso-

Madueño et al. 2017, SEMARNAT 2018). These data indicate that pine sawdust is an abundant material that could support the production of activated carbon.

Sawdust is the principal residue in the sawmill industry and is mainly used as fuel and in farm cleaning. However, it is frequently left in the field due to complex transportation logistics, thereby creating disposal and management problems (Fregoso-Madueño et al. 2017). Therefore, it is necessary to develop new sustainable alternatives for the use of agroforestry waste.

The use of agroforestry waste for the production of adsorbent materials is part of the principles of the circular economy. This approach promotes the valorization of waste as a resource, contributing to the closure of material and energy cycles and reducing the environmental impacts associated with its inadequate disposal by proposing more sustainable and resilient production models with fewer negative externalities (Smol 2023).

The aim of the current study was to evaluate the potential of activated carbon prepared from pine sawdust for removing EE2 from a water model.

MATERIALS AND METHODS

Chemical characterization of pine sawdust

Pine sawdust was obtained in December 2021 from the Santana Beltrán sawmill in Durango, Mexico. This sawmill came from different species of *Pinus*, such as *P. duranguensis*, *P. cooperi*, *P. teocote*, *P. leiophyla*, *P. engelmannii*, *P. arizonica*, *P. ayacahuite*, and *P. lumholtzii* (Rzedowski 1983, Valles-Gándara and Valadez-Castro 2006, Navar-Cháidez and González-Elizondo 2009, de la Paz-Pérez and Dávalos-Sotelo 2016).

Pine sawdust was dried (100 ºC for 24 h) and stored until use. The pine sawdust was chemically characterized according to the protocol of the Chihuahua (Mexico) Unit of the Centro de Investigación en Materiales Avanzados (Center for Research in Advanced Materials, CIMAV), using a Thermo Scientific FlashSmart Elemental Analyzer. Pine sawdust was also analyzed in a thermogravimetric analyzer Q600 under the following conditions: argon atmosphere with 50 cm^3/min flow, and heating ramp (10 ºC/min) from room temperature to 600 ºC, subsequently changing the atmosphere to air and heating up to 800 ºC.

Information about the functional groups present in the pine sawdust was obtained from a Fourier transform infrared spectroscopy (FTIR) analysis, using a Shimadzu spectrometer model IR Affinity 1S with an attenuated total reflection accessory (ATR) Smiths model Quest, in a scan window from 4000 to 400 cm^{-1}.

Preparation of activated carbons

Activated carbons were prepared according to Molina (2018). Pine sawdust (100 g) was pyrolyzed in a nitrogen atmosphere with a heating ramp of 20 ºC/min until 800 ºC for 30 min. At this point, a sample named thermally activated carbon (TAC) was collected to compare the removal efficiency of EE2 with that of chemically activated carbons. Then, samples were chemically activated by immersion in H_3PO_4 (85%) for 16 h using two impregnation ratios (IR) at room temperature (w/w). An IR of 0.5 was used to prepare activated carbon 1 (AC1), whereas an IR of 1.0 was used to prepare activated carbon 2 (AC2). Subsequently, the activated carbons obtained were washed once with acidulated water (HCl 0.1 M) and then with distilled water until a residual solution with pH 6.5 was obtained. TAC, AC1, and AC2 were dried at 100 ºC for 24 h, ground in an agate mortar, and sieved through a mesh No. 250 (0.062 mm aperture). Yield was determined based on initial and final weight difference. At the end of each activation type (yield % = [weight of activated carbon obtained/weight of pine sawdust used] × 100).

Physical and chemical characterization of activated carbon

The elemental analysis and surface morphology of the activated carbons were carried out following the protocols of CIMAV-Monterrey by energy dispersive spectroscopy (EDS), using a scanning electron microscopy (SEM) with a JEOL microscope, model JSM-6010PLUS/LA operating at 15 kV using secondary electron signal.

Information about functional groups present on the activated carbons was obtained from FTIR analysis, using a Thermo Scientific spectrometer model Nicolet iS50 and an ATR accessory. The wavelength was recorded from 4000 to 400 cm^{-1}.

Information about the crystalline phase of the activated carbons was acquired using an X-ray Panalytical Empyrean diffractometer (XDR), whose source was a Cu anode with λ = 1.5405 Aº, and the scanning angular range was from 5 to 90º. The obtained diffractograms were compared with the graphite diffraction pattern, which is used to compare the structures of activated carbon with those of graphite. N_2 adsorption-desorption isotherms were determined

at the condensation point of nitrogen (77.35 K) using a Quantachrome surface analyzer model Nova 4200e. The activated carbons were previously degassed for 12 h at 250 ºC under vacuum. The specific surface area (ES) was evaluated using the Brunauer-Emmett-Teller (BET) multipoint technique (Brunauer et al. 1938). The total pore volume (V_{tot}) was determined from the amount of N_2 adsorbed at relative pressure (P/P_o) around 0.99. The average pore diameter (D_p) was calculated from the relation: $D_p = 4V_{tot}/ES$. The monolayer capacity (V_m) was calculated from the relation: $V_m = 1/(b \times C)$ (b and C were obtained from a multi-point BET plot).

EE2 removal analysis

The evaluation of 17-α-ethinylestradiol removal by activated carbon was carried out using 400 mg/L of EE2 (≥ 98% pure, Sigma-Aldrich) in water-ethanol (7:3, v/v).

The optimization of adsorbent mass was performed using 68, 400, 1200, 2000, and 2331 mg/L of activated carbon in 10 mL of water-ethanol (7:3, v/v), while pH levels of 1.7, 3, 6, 9, and 10.2 were used for pH optimization in 10 mL of the same water-ethanol model. Both the activated carbon concentrations and pH values were selected from a statistical design in DATAtab (2025). The samples were shaken for 24 h at 250 rpm. Then, tubes were centrifuged for 5 min at 5000 rpm to separate activated carbon from the water system. Removal kinetics were constructed for the system of 2331 mg/L activated carbon, pH 6, registering the EE2 concentration at different contact times (0.5, 1.0, 2.0, 4.0, 8.0, 12.0, and 24.0 h). The EE2 concentration was determined by Flexar LC high-performance liquid chromatography with photodiode array plus detector (HPLC-PDA) and a C18 column, according to the method described by Linares (2019), using a standard curve of EE2 (area = 132 083 [EE2] – 3E + 07, coefficient of determination $R^2 = 0.974$, detection limit= 50.65 mg/L, limit of quantification = 153.49 mg/L). The contents were expressed as milligrams of EE2/L water-ethanol. The retention time (RT) of EE2 was 2.95 ± 0.25 min.

Pseudo-first order and pseudo-second order kinetic models were tested with the experimental data obtained to comprehend the kinetics of EE2 removal using TAC, AC1, and AC2 as adsorbents. Different initial concentrations of EE2 (300, 325, 350, 375, and 400 mg/L) were used to perform adsorption isotherm experiments with TAC, AC1, and AC2 (2331 mg/L) during 24 h. The results were modeled for two different models, Langmuir and Freundlich, in order to determine which is more suitable to represent the adsorption data.

Data analysis

All assays were performed on two independent pools per sample. Data were subjected to an analysis of variance (ANOVA), variables were considered significant when the P-value was less than 0.0500, and means were separated by percentage of EE2 removal, according to type and concentration of activated carbon used, as well as the pH of the water model, using the statistical program SigmaPlot 11.0. The coefficient of determination (R^2) was calculated to select the isothermal and kinetic model that best fit the data.

RESULTS AND DISCUSSION

Chemical characterization of pine sawdust

The elemental analysis revealed that pine sawdust contained 46.39% carbon and 5.74% hydrogen. Nitrogen and sulfur were not detected. Coronado (2016) obtained similar results for wood sawdust, except for the nitrogen and sulfur percentages (3.12 and 2%, respectively). According to the thermogravimetric analysis, pyrolysis was observed from 200 to 600 ºC, resulting in a loss of volatile components, which represented 72% of the mass of sawdust. Near 600 ºC, total fixed carbon was obtained with a percentage of 18.52, and when the combustion was achieved, a 2.7% of ash was obtained. The current results were in agreement with those of González (2017), who found that pine sawdust has a high carbon content and a low ash content, making it ideal for activated carbon production.

The FTIR spectrum of pine sawdust was similar to that of cellulose (**Fig. 1**), analyzed here as a reference, as expected, since cellulose is one of the main structural components of plants. The signal found at 3300 cm^{-1} corresponds to -OH elongation; the band at 2900 cm^{-1} represents a C-H elongation; peaks observed at 1730, 1600, and 1510 cm^{-1} were related to the C=O stretching; bands at 1450, 1420, 1365, and 1320 cm^{-1} were associated with C-H deformations. The signals at 1160, 1060, and 1020 cm^{-1} are related to the C-O elongation, whereas the band at 810 cm^{-1} could correspond to an aromatic substitution. These signals correspond mainly to alcohols, ethers, phenols, carboxylic acids, and ketones that have been related to lignocellulosic compounds detected in different types of plants, including timber species (Contreras-Valero et al. 2017, González 2017, Kan et al. 2017, Moya et al. 2017).

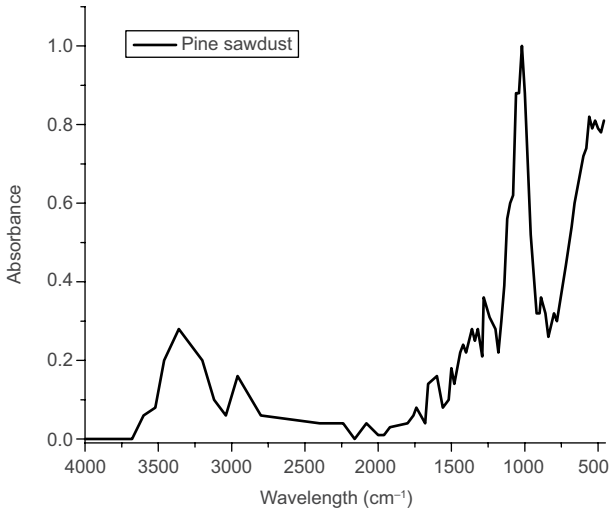

Fig. 1. Fourier transform infrared spectroscopy spectra of pine sawdust.

Activated carbon obtained

The yield percentages obtained were 18.0 ± 0.8 for TAC, 18.3 ± 0.6 for AC1, and 17.9 ± 1.3 for AC2. No significant differences were found. These results were consistent with those determined during the thermogravimetric analysis of pine sawdust related to the percentage of total fixed carbon. The yields of the three activated carbons are higher than those of pine sawdust obtained by González (2017) through physical activation (11.6%).

Physical and chemical characterization of activated carbon

The elemental composition of TAC, AC1, and AC2, revealed by EDS, is shown in **Table I**. The carbon percentages obtained were similar to those found by Patel et al. (2023) for activated carbons also prepared from pine sawdust (82-89%); however, TAC, AC1, and AC2 contained lower oxygen levels, which may be attributable to the activating agent used (H_3PO_4), since they used KOH, CO_2, and KOH + CO_2, reporting oxygen levels of 8-16%. The presence of oxygen in activated carbons is a desirable characteristic as it can promote adsorption mechanisms via the functional groups that it can form (Álvarez-Torrellas et al. 2016). Also, the absence of phosphorus in TAC and its presence in AC1 and AC2 were in agreement with the chemical activation using H_3PO_4 applied only to AC1 and AC2. Since AC1 and AC2 were activated with this acid, the presence of phosphorus is understood, though it is not commonly found in activated carbons (Vela-Carrillo et al. 2024) and may cause pore clogging (González 2017); however, the amount of this element was not significant in comparison to the presence of carbon and oxygen.

TABLE I. ELEMENTAL SEMI-QUANTIFICATION OF ACTIVATED CARBON BY ENERGY DISPERSIVE SPECTROSCOPY.

Element	TAC (%)	AC1 (%)	AC2 (%)
Carbon	89.26	90.19	90.54
Oxygen	8.69	7.12	6.97
Phosphorus	0.00	0.48	0.28

TAC: thermally activated carbon, AC1: chemically activated carbon with H_3PO_4 and IR of 0.5, AC2: chemically activated carbon with H_3PO_4 and IR of 1.0, IR: impregnation ratio.

A higher level of carbon was found in TAC, AC1, and AC2 (89.26, 90.19, and 90.54%, respectively) compared to pine sawdust (46.39%). Higher levels of carbon in activated carbons than in raw materials are expected as a consequence of suitable pyrolysis processes (Alvarado-Flores and Rutiaga-Quiñones 2018).

The TAC, AC1, and AC2 morphology, revealed by SEM (**Fig. 2**), suggests the presence of irregular, laminar and tubular structures with pores lower than 3 μm in diameter in their surfaces, which allow activated carbons to increase their specific surface area; in addition, it exhibits roughness, which is one of the desirable characteristics in an activated carbon, as Rovani et al. (2016) found in activated carbon elaborated from coffee and wood wastes.

According to the FTIR analysis (**Fig. 3**), most of the signals observed in the spectrum of pine sawdust decrease or disappear in the spectrum of activated carbons, which is a result of the activation process due to the decomposition of organic matter (Kan et al. 2017), as activation breaks the less stable bonds, releasing the volatile fraction of the precursor material; thus, a carbonaceous residue enriched in carbon aromatic rings is obtained (Pallarés et al. 2018). The bands found in TAC, AC1, and AC2 are listed in **table II**, which coincide with bands found in other activated carbons prepared from other materials, such as mineral coal, coffee, apple and citrus residues, rice and coconut shells, sugar cane, agave bagasse, and different types of sawdust (Acevedo et al. 2016, Rovani et al. 2016, González 2017, Caglar et al. 2024, Mousazadeh et al. 2024, Vela-Carrillo et al. 2024).

The activated carbon obtained in the current study mostly presents signals corresponding to the functional groups C-H in aliphatic structures, C=C in aromatic compounds, and -OH groups. These groups can

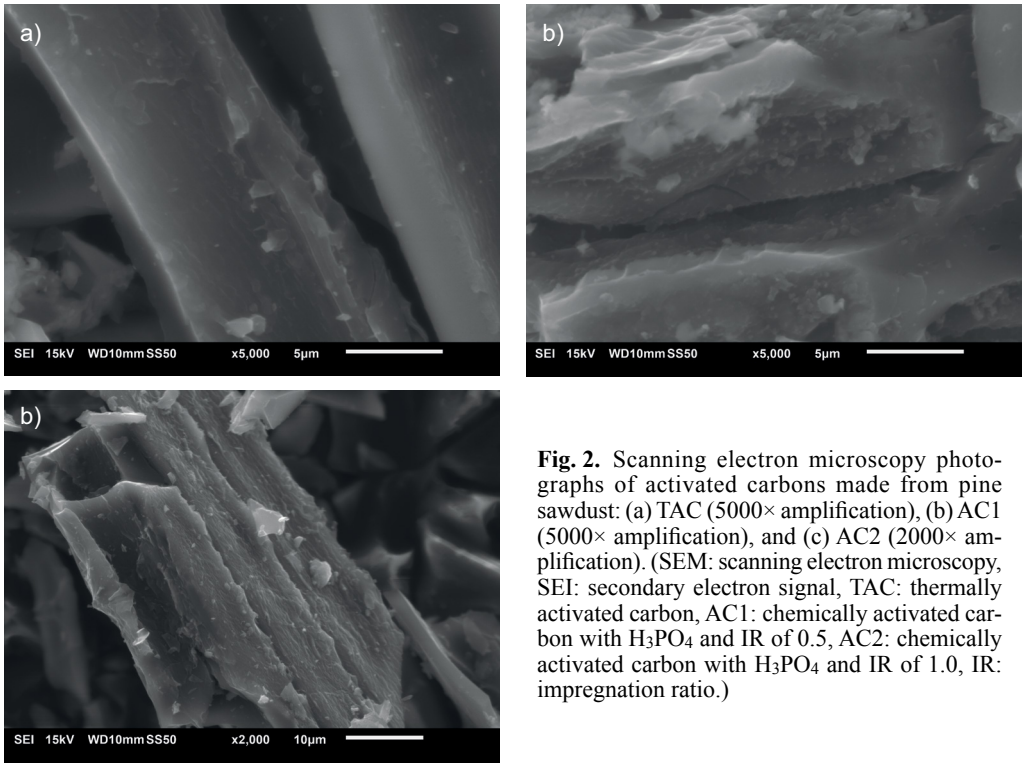

Fig. 2. Scanning electron microscopy photographs of activated carbons made from pine sawdust: (a) TAC (5000× amplification), (b) AC1 (5000× amplification), and (c) AC2 (2000× amplification). (SEM: scanning electron microscopy, SEI: secondary electron signal, TAC: thermally activated carbon, AC1: chemically activated carbon with H_3PO_4 and IR of 0.5, AC2: chemically activated carbon with H_3PO_4 and IR of 1.0, IR: impregnation ratio.)

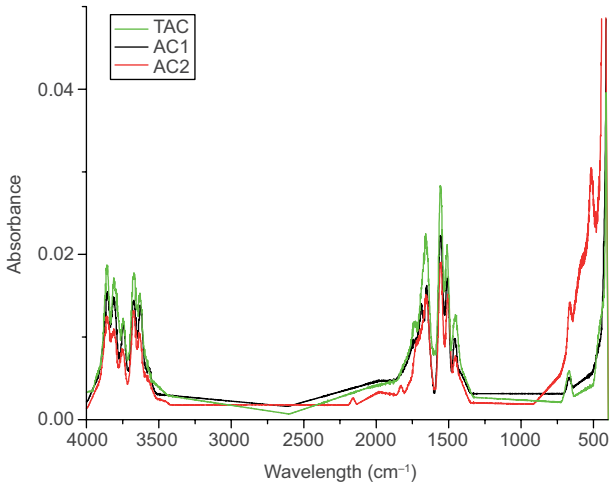

Fig. 3. Fourier transform infrared spectroscopy spectra of prepared activated carbons. (TAC: thermally activated carbon, AC1: chemically activated carbon with H_3PO_4 and IR of 0.5, AC2: chemically activated carbon with H_3PO_4 and IR of 1.0, IR: impregnation ratio.)

allow TAC, AC1, and AC2 to form hydrogen bonds or π-π electron-donor-acceptor (EDA) interactions with EE2 (Álvarez-Torrellas et al. 2016). In AC1 and AC2, C=O groups were observed, which could be formed due to chemical activation with H_3PO_4, as this acid is capable of promoting the formation of acid groups on the surface of carbons (González 2017). It was found that H_3PO_4 contributes to the formation of acidic functional groups, such as carboxylic acids, phenols, and lactones, and to the formation of basic functional groups, such as carbonyls and quinones (Vela-Carrillo et al. 2024).

The diffractograms obtained for TAC, AC1, and AC2 (**Fig. 4**), compared with the graphite diffraction pattern, indicated similarities to the crystallographic planes 002 and 111. This suggests that the crystal systems of the activated carbons are related to the irregular, laminar, and tubular structures observed by SEM. Plane 002 was also observed by Kan et al. (2017) in an activated carbon made from tea waste,

TABLE II. FOURIER TRANSFORM INFRARED SPECTROSCOPY BANDS OBSERVED IN ACTIVATED CARBONS.

TAC		AC1		AC2	
Wavelength (cm^{-1})	Functional group	Wavelength (cm^{-1})	Functional group	Wavelength (cm^{-1})	Functional group
3858, 3808, 3746, 3672, and 3628	-OH stretching	3858, 3808, 3746, 3672, 3628, and 3573	-OH stretching	3858, 3808, 3751, 3672, 3636, and 3576	-OH stretching
				2160	RC≡CH stretching
		1746 and 1690	C=O stretching	1831	C=O stretching
1658, 1556, and 1509	C=C elongation in aromatic compounds	1652, 1556, and 1509	C=C elongation in aromatic compounds	1658, 1553, and 1504	C=C elongation in aromatic compounds
1452	C-H deformation in aliphatic structures	1452	C-H deformation in aliphatic structures	1452	C-H deformation in aliphatic structures
669 and 414	Out-of-plane C-H deformation in aromatic compounds	667 and 414	Out-of-plane C-H deformation in aromatic compounds	664, 517, and 420	Out-of-plane C-H deformation in aromatic compounds

TAC: thermally activated carbon, AC1: chemically activated carbon with H_3PO_4 and IR of 0.5, AC2: chemically activated carbon with H_3PO_4 and IR of 1.0, IR: impregnation ratio.

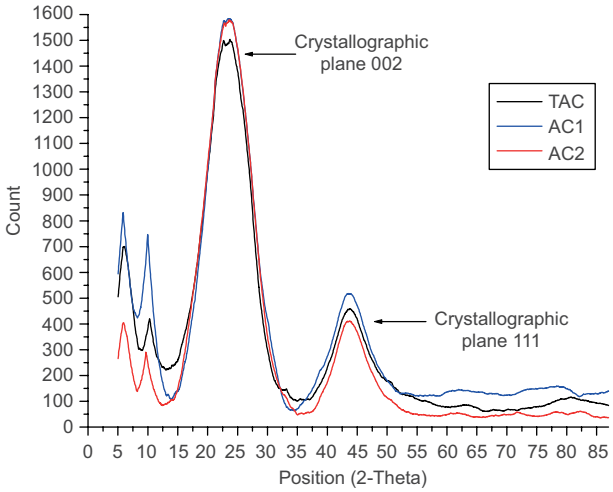

Fig. 4. Comparison of TAC, AC1, and AC2 diffractograms. (TAC: thermally activated carbon, AC1: chemically activated carbon with H_3PO_4 and IR of 0.5, AC2: chemically activated carbon with H_3PO_4 and IR of 1.0, IR: impregnation ratio).

indicating a stacked structure. Plane 111 is related to face-centered cubic crystalline structures.

The nitrogen adsorption and desorption isotherms of TAC, AC1, and AC2 can be seen in **figure 5**. According to the Brunauer-Deming-Deming-Teller (BDDT) classification, the isotherms correspond to type I, indicating that adsorption occurs in a monolayer at relatively low pressures, leading to saturation of the adsorbate in a shorter time, which is due to enhanced adsorbent-adsorptive interactions in narrow pores, slit-like pores, or narrow channels such as pores of molecular dimensions. Thus, type I is related to solid materials that present narrow micropores (of width less than 1 nm), wider micropores in sizes minor than 2 nm in diameter and narrow mesopores (less than 2.5 nm wide) with relatively small external surfaces (Brunauer et al. 1940, Thommes et al. 2015). Due to minor pore size, it could be inferred that they have narrow necks, probably with ink-bottle pore shape, so the mechanism of desorption includes cavitation (Thommes et al. 2015).

The shape of hysteresis was classified as H4. This loop is given by non-rigid aggregates of plate-like particles, but also if the pore network consists of macropores, which are not completely filled with pore condensate, and it is often found in micro-mesoporous carbons (Thommes et al. 2015). In these isotherms, a high value of parameter C was obtained (greater than 150), which means, according to the BET theory, that adsorption is related to filling of narrow micropores.

The type of isotherms found here agrees with those found by Pimentel et al. (2024) for activated carbon made from *Pinus radiata* and supports the proposal of Üner and Bayrak (2018), who stated that the adsorption and desorption isotherms with N_2 for activated carbons are generally type I.

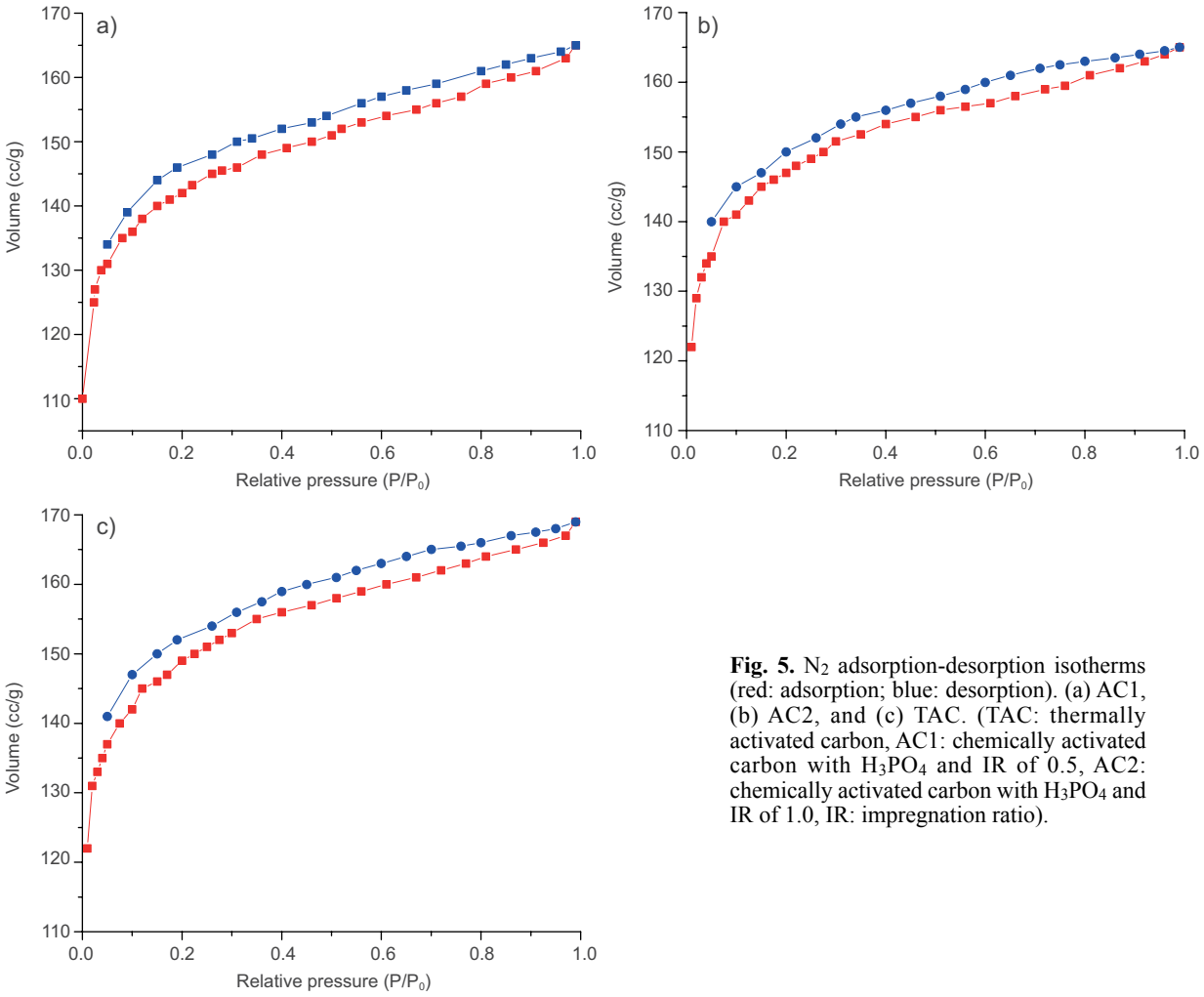

Fig. 5. N_2 adsorption-desorption isotherms (red: adsorption; blue: desorption). (a) AC1, (b) AC2, and (c) TAC. (TAC: thermally activated carbon, AC1: chemically activated carbon with H_3PO_4 and IR of 0.5, AC2: chemically activated carbon with H_3PO_4 and IR of 1.0, IR: impregnation ratio).

Activated carbon-specific surface depends on the precursor material, and type and conditions of activation used for its preparation (Pallarés et al. 2018, Arévalo and Reátegui 2020, Cabrera et al. 2020); therefore, a high variation in the physical and chemical properties of activated carbons can be found. The ES values obtained in the current study (estimated by the BET method) were 543.0 m^2/g (TAC), 566.1 m^2/g (AC1), and 571.7 m^2/g (AC2); the differences among them were not significant ($p = 0.2386$). **Table III** presents the textural parameters measured in the samples (V_{TOT} = 0.153 cm^3/g, Dp = 1.07 to 1.127 nm, and V_m = 0.1512 to 0.1639 mL/g), indicating a dominant microporous surface in the activated carbons obtained from pine sawdust waste. This porous structure is consistent with materials that are effective in the adsorption of small to medium-sized molecules, such as hormones, since the micropores provide a high number of adsorption sites per unit of mass, favoring Van Der Waals interactions and, in the presence of functional groups, more specific interactions (Asheghmoalla and Mehrvar 2024, Lang et al. 2024). The slight variations between TAC, AC1, and AC2 in Dp and V_m could be attributed to differences in activation conditions.

TABLE III. TEXTURAL PROPERTIES OF ACTIVATED CARBONS.

	TAC	AC1	AC2
V_{TOT} (cm^3/g)	0.153	0.153	0.153
Dp (nm)	1.127	1.081	1.07
V_m (mL/g)	0.1512	0.1610	0.1639

TAC: thermally activated carbon, AC1: chemically activated carbon with H_3PO_4 and IR of 0.5, AC2: chemically activated carbon with H_3PO_4 and IR of 1.0, IR: impregnation ratio, V_{TOT}: total pore volume, Dp: average pore diameter, V_m: monolayer capacity.

Phosphoric acid is one of the most widely used chemical activators because, in the presence of heat, it generates activated carbons having both high porosity and surface area (Vela-Carrillo et al. 2024). In the current study, the use of heat was avoided, as heat generates corrosive atmospheres. Instead, two IR (0.5 and 1.0) combined with H_3PO_4 at room temperature for 16 h (a prolonged impregnation time). The results showed that impregnation carried out in this manner generated no significant changes in the ES of the activated carbons obtained compared to the thermally activated carbon, which generates an adequate ES without the use of many chemicals and without generating much waste that pollute the environment and harm humans. Even so, the ES values obtained here for TAC, AC1, and AC2 were higher (543.0, 566.1 and 571.7 m^2/g, respectively) than that reported for an adsorbent made with a mixture of coffee, sawdust and oil, under similar activation conditions (16.5 m^2/g) by Rovani et al. (2014). The ES values obtained for TAC, AC1, and AC2 suggest that pine sawdust has an important potential to produce activated carbons having high specific surface areas, which can favor the removal potential of EE2.

Adsorption analysis

Significant differences in EE2 adsorption between AC1, AC2, and TAC can be appreciated in **table IV**. TAC was removed between 2.04 and 22.22%, AC1 between 1.71 and 26.53%, whereas AC2 was between 1.23 and 26.92%. The significant interaction between activated carbon concentration and pH (TAC: $p = 0.006$; AC1: $p = 0.001$; AC2: $p = 0.001$) indicated that the removal effect of the different activated carbon

TABLE IV. 17-α-ETHINYLESTRADIOL (EE2) REMOVAL PERCENTAGES*.

[Carbon] (mg/L)	pH	EE2 removal (%)		
		TAC	AC1	AC2
68	1.7	4.96 ± 2.62	1.77 ± 0.40	2.17 ± 0.24
	3	4.14 ± 1.80	2.64 ± 0.21	2.78 ± 0.02
	6	7.10 ± 0.08	5.24 ± 2.47	9.46 ± 4.06
	9	3.53 ± 1.16	2.70 ± 0.09	2.03 ± 0.09
	10.2	3.44 ± 0.34	3.21 ± 0.06	2.81 ± 0.13
400	1.7	4.54 ± 2.50	2.26 ± 0.16	2.91 ± 0.00
	3	3.46 ± 1.60	1.71 ± 0.14	1.50 ± 0.43
	6	4.32 ± 2.39	1.92 ± 0.09	6.48 ± 0.79
	9	2.04 ± 0.35	2.58 ± 0.18	1.23 ± 0.87
	10.2	5.55 ± 1.79	3.80 ± 0.65	3.19 ± 0.20
1200	1.7	6.61 ± 3.36	3.68 ± 0.56	4.12 ± 0.93
	3	4.92 ± 1.29	3.30 ± 0.03	3.05 ± 0.05
	6	7.64 ± 0.07	7.61 ± 3.16	12.94 ± 0.57
	9	3.66 ± 1.55	2.61 ± 0.11	2.74 ± 0.17
	10.2	4.72 ± 1.82	3.30 ± 0.57	2.28 ± 0.26
2000	1.7	5.00 ± 2.76	4.32 ± 0.11	4.02 ± 0.24
	3	5.44 ± 2.95	2.90 ± 0.56	2.09 ± 0.28
	6	9.01 ± 1.36	5.41 ± 2.85	14.50 ± 1.32
	9	4.55 ± 3.22	3.39 ± 0.02	5.16 ± 2.63
	10.2	3.96 ± 0.63	4.71 ± 0.77	3.70 ± 0.12
2331	1.7	4.86 ± 3.38	3.65 ± 0.09	4.62 ± 0.16
	3	5.52 ± 2.42	4.02 ± 0.04	5.64 ± 2.21
	6	22.22 ± 5.21	26.53 ± 0.39	26.92 ± 0.16
	9	3.03 ± 1.62	2.95 ± 0.16	2.15 ± 0.25
	10.2	3.28 ± 0.51	3.33 ± 0.01	3.56 ± 0.01

*The evaluation of EE2 removal was carried out at 24 h.
[Carbon]: activated carbon concentration, TAC: thermally activated carbon, AC1: chemically activated carbon with H_3PO_4 and IR of 0.5, AC2: chemically activated carbon with H_3PO_4 and IR of 1.0, IR: impregnation ratio.

concentrations depends on the pH value of the water model. Most of the concentrations of either AC1, AC2, or TAC removed higher amounts of EE2 at pH 6.

The pH influences the adsorption process because it depends on the chemical species of the adsorbate and on the surface charge of the activated carbon (Moura et al. 2018). In the present study, it was observed that at pH 1.7, 3, 9, and 10.2, there was less EE2 removal; this means that an intense ionization of EE2 did not occur (the EE2 dissociation constant is 10.24), which is why it was considered that a neutral form of EE2 molecule predominated in the different pH tests. Therefore, it was deduced that in this study, only the charge effect on the surface of the activated carbons influenced the adsorption process. As observed in **table IV**, EE2 removal percentages are greater at pH 6, so it was concluded that the surface charge of the activated carbons was neutral. Moura et al. (2018) also found that the charge effect on the surface of the activated carbons made with macauba (*Acrocomia aculeata*) residues was of greater relevance in the adsorption process of EE2 and proposed that by having favorable results under these conditions (lack of ionization of EE2, neutral charge on the activated carbons surfaces and higher EE2 adsorption at pH 6), the most likely mechanism of interaction in the adsorption was the π-π interaction between the aromatic structures of activated carbon layers and aromatic structures of EE2.

Either AC1, AC2, or TAC at 2331 mg/L displayed the highest potential to remove EE2. This may be explained by the fact that, at this concentration, many more adsorption sites were available than at the lower concentrations, thereby improving EE2 removal.

The results of the ANOVA performed to select which of the three activated carbons at 2331 mg/L and pH 6 had the highest capacity for removing EE2 revealed no significant differences between them ($p = 0.200$), which agrees with the non-significant differences found in porosity and ES (**Fig. 2**) among TAC, AC1, and AC2.

The percentages achieved in the removal of EE2 by TAC (22.22%), AC1 (26.53%) and AC2 (26.92%) were lower than those reported by other authors (> 90%) for the same hormone (Rovani et al. 2014, Moura et al. 2018). Nevertheless, it is important to comment that in the current study, the concentration of EE2 (400 mg/L) used and the concentrations of activated carbons (2331 mg/L) were higher than in the studies carried out by Rovani et al. (2014), in which he used 2 mg/L of EE2 and 1500 mg/L of activated carbon. This means that in this study, 5.82 mg/L of activated carbon is used to remove 1 mg/L of EE2 while Rovani et al. (2014) used a ratio of 750 mg/L of activated carbon to remove 1 mg/L of EE2. Therefore, the activated carbon obtained in the present work demonstrated more efficiency to remove a greater concentration of EE2.

The effect of time in EE2 removal is shown in **figure 6**. Although the three activated carbon samples achieved similar removal percentages, these percentages were reached at different times. TAC reached equilibrium after 12 h, while AC1 and AC2 reached equilibrium after only 2 h. This important difference may be due to functional groups generated on the surface of the carbons chemically activated with H_3PO_4 that favor chemical bonds like Van der Waals forces or covalent bonds in such a way that the adsorption process was carried out faster. The parameters calculated in pseudo-first order and pseudo-second order kinetic models are contained in **table V**. From the results, it could be deduced that the pseudo-second order model could explain the adsorption processes better than the pseudo-first order model, because of higher R^2 values. Furthermore, the equilibrium adsorption capacity (q_e) calculated by this model revealed values similar to experimental q_e. The reaction rate constant (K_2) was higher in AC1 (0.0028 g/mg/min) than in TAC and AC2 (0.0002 and 0.0008 g/mg/min, respectively), which indicated that the EE2 adsorption is faster with AC2. The adsorption rate of EE2 determines the residence time of the adsorption process, which is important for water treatment, as shorter residence times yield faster treatment. The pseudo-second-order model indicated that adsorption was primarily controlled by chemical adsorption, which could be attributed to the functional groups present in TAC, AC1, and AC2 (Osman et al. 2023).

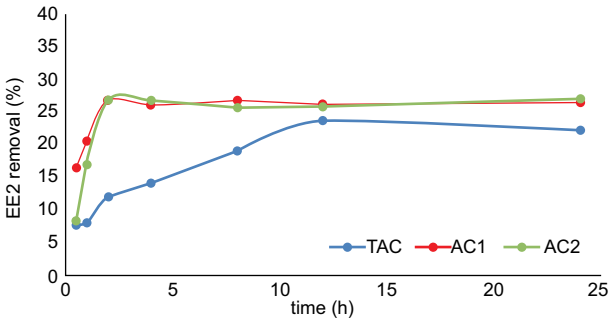

Fig. 6. Effect of time on 17-α-ethinylestradiol (EE2) removal with three activated carbons. (TAC: thermally activated carbon, AC1: chemically activated carbon with H_3PO_4 and IR of 0.5, AC2: chemically activated carbon with H_3PO_4 and IR of 1.0, IR: impregnation ratio).

TABLE V. KINETIC PARAMETERS OF 17-α-ETHINYLESTRADIOL ADSORPTION MODELS.

Adsorbent	Pseudo-first order		Pseudo-second order	
	Parameter	Value	Parameter	Value
TAC	Experimental q_e = 40.61 (mg/g)			
	q_e (mg/g)	38.72	q_e (mg/g)	40.81
	K_1 (min^{-1})	0.2708	K_2 (g/mg/min)	0.0002
	R^2	0.9378	R^2	0.9862
AC1	Experimental q_e = 46.09 mg/g			
	q_e (mg/g)	50.96	q_e (mg/g)	45.87
	K_1 (min^{-1})	1.8907	K_2 (g/mg/min)	0.0028
	R^2	0.9794	R^2	0.9997
AC2	Experimental q_e = 45.89 mg/g			
	q_e (mg/g)	69.29	q_e (mg/g)	46.72
	K_1 (min^{-1})	1.8907	K_2 (g/mg/min)	0.0008
	R^2	0.9607	R^2	0.9978

TAC: thermally activated carbon, AC1: chemically activated carbon with H_3PO_4 and IR of 0.5, AC2: chemically activated carbon with H_3PO_4 and IR of 1.0, IR: impregnation ratio, $\mathbf{q}_e$: equilibrium adsorption capacity, K_1: pseudo-first order rate constant, K_2: pseudo-second order rate constant, R^2: determination coefficient.

After modeling both Langmuir and Freundlich equations, it was obtained that the Langmuir isotherm was more suitable to describe the adsorption process in TAC (R^2 = 0.9848), AC1 (R^2 = 0.9819), and AC2 (R^2 = 0.9822) (**Table VI**). These results coincide with those found by Moura et al. (2018) to explain the equilibrium relation between EE2 and activated carbon made with macauba residues. The Langmuir isotherm indicated that the adsorbent's adsorption sites are homogeneous and well distributed, enabling monolayer adsorption (Zhang et al. 2020). The results also indicated the maximum adsorption capacities of TAC, AC1, and AC2 (qmax = 15.55, 23.47, and 16.75 mg g–1, respectively), with AC1 exhibiting the highest capacity. The q_{max} calculated in this work was greater than that reported by Moura et al. (2018) for the same hormone (0.104 mmol/g). The Langmuir constant (K_L) depends on the free energy of adsorption so, a greater value of K_L means that saturation is achieved at lower values of equilibrium concentrations. This parameter is higher for EE2 with AC2 (K_L = 0.002423 mg/L) than for TAC and AC1 (K_L = 0.002310 and 0.002076 mg/L, respectively), suggesting a stronger interaction with the AC2 surface.

TABLE VI. PARAMETERS OF THE LANGMUIR ADSORPTION ISOTHERMS.

	TAC	AC1	AC2
R^2	0.9848	0.9819	0.9822
q_{max} (mg/g)	15.55	23.47	16.75
K_L (mg/L)	0.002310	0.002076	0.002423

TAC: thermally activated carbon, AC1: chemically activated carbon with H_3PO_4 and IR of 0.5, AC2: chemically activated carbon with H_3PO_4 and IR of 1.0, IR: impregnation ratio, R^2: determination coefficient, q_{max}: maximum adsorption capacity, K_L: Langmuir constant.

CONCLUSIONS

Pine sawdust is a viable material for producing activated carbon with appropriate properties (yield, elemental composition, surface morphology, surface chemistry, crystalline phase, and specific surface area) for removing EE2, whose presence in aquatic systems and wastewater has emerged as a significant environmental and health concern. Production of activated carbon from pine sawdust can contribute to the development of management programs for this residue, reducing soil contamination. Thus, converting agroforestry waste into activated carbon constitutes a sustainable strategy that integrates advanced water treatment with responsible waste management, promoting an environmentally sustainable development

model that is scientifically justifiable and aligned with global ecological preservation objectives.

The method presented here for preparing activated carbon is low-cost, easy to implement and operate, and effective for removing EE2. The three activated carbons obtained showed no significant differences in their capacity for removing EE2; however, preparation of TAC was simpler and shorter than the preparation of AC1 and AC2, because it required no chemical reagents, corrosive atmospheres during heat treatment, or long impregnation times. Therefore, given the simplicity and low cost of the preparation procedure, the yield, and the capacity to remove EE2, TAC represents an adequate alternative. Although it took longer to reach the highest EE2 removal capacity, this does not indicate problems with its functionality or its application as a tertiary unit operation in water treatment. EE2 removal in this study demonstrated the potential of the adsorption process for emerging contaminants.

REFERENCES

Acevedo S., Galicia L., Plaza E., Atencio R., Rodríguez A. and González E. (2016). Carbón activado preparado a partir de carbón mineral bituminoso activado con hidróxido de potasio. Revista Técnica de la Facultad de Ingeniería, Universidad del Zulia 39 (2), 064-070.

Ali H., Yasir M., Masar M., Suly P., Sopik T., Zubair M., Monteiro O. C., Machovsky M., Sedlarik V. and Kuritka I. (2024). Titanium dioxide and halloysite loaded polylactic acid-based membrane continuous flow photoreactor for 17α-ethinylestradiol (EE2) hormone degradation: Optimization, kinetics, mechanism, and reusability study. Catalysis Today 432, 114602. https://doi.org/10.1016/j.cattod.2024.114602

Alvarado-Flores J.J. and Rutiaga-Quiñones J.G. (2018). Estudio de cinética en procesos termogravimétricos de materiales lignocelulósicos. Maderas. Ciencia y Tecnología 20 (2), 221-238. https://doi.org/10.4067/s0718-221x2018005002601

Álvarez-Torrellas S., Rodríguez A., Ovejero G. and García J. (2016). Comparative adsorption performance of ibuprofen and tetracycline from aqueous solution by carbonaceous materials. Chemical Engineering Journal 283, 936-947. https://doi.org/10.1016/j.cej.2015.08.023

Arévalo F.H. and Reátegui K. (2020). Calidad y rendimiento del carbón activado de la cáscara del fruto de calabaza (*Cucurbita ficifolia*) obtenido por método químico. Revista Forestal del Perú 35 (1), 21-30. https://doi.org/10.21704/rfp.v35i1.1473

Asheghmoalla M. and Mehrvar M. (2024). Adsorption of a multicomponent pharmaceutical wastewater on charcoal-based activated carbon: Equilibrium and kinetics. Water 16 (15), 2086. https://doi.org/10.3390/w16152086

Brunauer S., Emmett P.H. and Teller E. (1938). Adsorption of gases in multimolecular layers. Journal of the American Chemical Society 60 (2), 309-319. https://doi.org/10.1021/ja01269a023

Brunauer S., Deming L.S., Deming W.E. and Teller E. (1940). On a theory of the Van der Waals adsorption of gases. Journal of the American Chemical Society 62 (7), 1723-1732. https://doi.org/10.1021/ja01864a025

Bundy M.M., Doucette W.J., McNeill L. and Ericson J.F. (2007). Removal of pharmaceuticals and related compounds by a bench-scale drinking water treatment system. Journal of Water Supply: Research and Technology 56 (2), 105-115. https://doi.org/10.2166/aqua.2007.091

Cabrera O., Bautista L., Ortega Y., Cabrera D. and Cuello M. (2020). Obtención de carbón activado a partir de la cáscara del coco (*Cocos nucífera* L) y su evaluación en la remoción de residuos líquidos coloreados. UT Ciencia 7 (3), 148-159.

Caglar A., Kaya S., Saka C., Yildiz D. and Kivrak H. (2024). Investigation of electrooxidation and methanolysis of sodium borohydride on activated carbon supported Co catalysts from poplar sawdust. International Journal of Hydrogen Energy 75, 171-178. https://doi.org/10.1016/j.ijhydene.2024.01.083

Contreras-Valero Y., Cardona-Rodríguez Y. and Torres-Sánchez D.A. (2017). Estudio térmico e infrarrojo de cinco tipos de madera comercializadas en norte de Santander, para su posible uso como fuente de energía. Respuestas 22 (2), 36-47. https://doi.org/10.22463/0122820x.1173

Coronado J.P. (2016). Estimación de los parámetros cinéticos de un aserrín mediante la técnica de análisis termogravimétrico (TGA). B.Sc. thesis. Facultad de Ingeniería, Universidad de los Andes, Bogotá, Colombia, 30 pp.

DATAtab Team (2025). DATAtab: online statistics calculator [online]. https://datatab.net/statistics-calculator/design-of-experiments 09/09/2024

De la Paz-Pérez C. and Dávalos-Sotelo R. (2016). Anatomía de la madera de seis especies de *Pinus* (Pinaceae) del estado de Durango, México. Madera y Bosques 22 (3), 113-132. https://doi.org/10.21829/myb.2016.2231460

Fregoso-Madueño J.N., Goche-Télles J.R., Rutiaga-Quiñones J.G., González-Laredo R.F., Bocanegra-Salazar M. and Chávez-Simental J.A. (2017). Usos alternativos de los desechos de la industria del aser-

río. Revista Chapingo Serie Ciencias Forestales y del Ambiente 23 (2), 243-260. https://doi.org/10.5154/r.rchscfa.2016.06.040

Gogoi A., Mazumder P., Tyagi V.K., Tushara G.G., An A.K. and Kumar M. (2018). Occurrence and fate of emerging contaminants in water environment: A review. Groundwater for Sustainable Development 6, 169-180. https://doi.org/10.1016/j.gsd.2017.12.009

González B. (2017). Desarrollo de carbón activado a partir de desechos agroindustriales con aplicación en adsorción de arsénico. B.Sc. thesis. Facultad de Ciencias Químicas y Matemáticas, Universidad de Chile, Santiago, 93 pp.

Kan Y., Yue Q., Li D., Wu Y. and Gao B. (2017). Preparation and characterization of activated carbons from waste tea by H_3PO_4 activation in different atmospheres for oxytetracycline removal. Journal of the Taiwan Institute of Chemical Engineers 71, 494-500. https://doi.org/10.1016/j.jtice.2016.12.012

Lang J., Bednárek J., Ritz M., Kormunda M., Zelenka T., Vastyl M., Gavlová A., Kolská Z. and Férová M. (2024). Materials Advances 5, 6458-6468. https://doi.org/10.1039/D4MA00141A

Linares S.A. (2019). Estudio de adsorción-desorción y degradación de 17-α- etinilestradiol (EE2) en suelos tratados con biosólidos. B.Sc. thesis. Facultad de Ciencias Químicas y Farmacéuticas, Universidad de Chile, Santiago, 67 pp.

Molina J.M. (2018). Obtención de carbón activado a partir de residuos del proceso de elaboración de mezcal y evaluación en la eficiencia de remoción de contaminantes en vinazas. M.Sc. thesis. Centro Interdisciplinario de Investigación para el Desarrollo Integral Regional-Unidad Durango, Instituto Politécnico Nacional, Durango, México, 73 pp.

Moura F.C.C., Rios R.D.F. and Galvão B.R.L. (2018). Emerging contaminants removal by granular activated carbon obtained from residual macauba biomass. Environmental Science and Pollution Research 25, 26482-26492. https://doi.org/10.1007/s11356-018-2713-8

Mousazadeh B., Mohammadi N. and Khosravi-Nikou M.R. (2024). Synthesis and characterization of porous activated carbons derived from lotus nut and their performance for CO_2 adsorption. International Journal of Environmental Science and Technology 21, 5379-5394. https://doi.org/10.1007/s13762-023-05435-1

Moya R., Salas C., Quesada J., Rodríguez A., Gaitán J., Puente A. and Vega J. (2017). Torrefacción del aserrín de cinco tipos de maderas de Costa Rica para aumentar el contenido energético (documento I), código de proyecto: 1401057. Informe Final de Proyecto de Investigación. Escuela de Ingeniería Forestal, Centro de Investigación en Innovación Forestal, Vicerrectoría de Investigación y Extensión, Instituto Tecnológico de Costa Rica, 111 pp.

Navar-Cháidez J. and González-Elizondo S. (2009). Diversidad, estructura y productividad de bosques templados de Durango, México. Polibotánica (27), 71-87.

Oropesa A.L. (2008). Disruptores endocrinos en el medio ambiente: caso del 17-α-etinil-estradiol. Observatorio Medioambiental 11, 63-76.

Oropesa A., Moreno J. and Gómez L. (2017). Lesiones histopatológicas en peces originadas por la exposición a contaminantes emergentes: recopilando y analizando datos. Revista de Toxicología 34, 99-108.

Osman A.I., Ayati A., Farghali M., Krivoshapkin P., Tanhaei B., Karimi-Maleh H., Krivoshapkina E., Taheri P., Tracey C., Al-Fatesh A., Ihara I., Rooney D.W. and Sillanpaä M. (2023). Advanced adsorbents for ibuprofen removal from aquatic environments: A review. Environmental Chemistry Letters 22, 373-418. https://doi.org/10.1007/s10311-023-01647-6

Pallarés J., González-Cencerrado A. and Arauzo I. (2018). Production and characterization of activated carbon from barley straw by physical activation with carbon dioxide and steam. Biomass and Bioenergy 115, 64-73. https://doi.org/10.1016/j.biombioe.2018.04.015

Patel H., Weldekidan H., Mohanty A. and Misra M. (2023). Effect of physicochemical activation on CO_2 adsorption of activated porous carbon derived from pine sawdust. Carbon Capture Science and Technology 8, 100128. https://doi.org/10.1016/j.ccst.2023.100128

Pimentel C.H., Freire M.S., Gómez-Díaz D. and González-Álvarez J. (2024). Continuous adsorption of acid wood dyes onto an activated carbon prepared from pine sawdust. Applied Sciences 14 (2), 841. https://doi.org/10.3390/app14020841

Ramírez-Sánchez I.M., Martínez-Austria P., Quiroz-Alfaro M. A. and Bandala E.R. (2015). Efectos de los estrógenos como contaminantes emergentes en la salud y el ambiente. Tecnología y Ciencias del Agua 6 (5), 31-42.

Richardson S.D. and Ternes T.A. (2018). Water analysis: Emerging contaminants and current issues. Analytical Chemistry 90 (1), 398-428. https://doi.org/10.1021/acs.analchem.7b04577

Rovani S., Censi M.T., Pedrotti S.L., Lima É.C., Cataluña R. and Fernandes A.N. (2014). Development of a new adsorbent from agro-industrial waste and its potential use in endocrine disruptor compound removal. Journal of Hazardous Materials 271, 311-320. https://doi.org/10.1016/j.jhazmat.2014.02.004

Rovani S., Rodrigues A.G., Medeiros L.F., Cataluña R., Lima É.C. and Fernandes A.N. (2016). Synthesis and characterisation of activated carbon from agroindustrial waste. Preliminary study of 17β-estradiol removal from aqueous solution. Journal of Environmental

Chemical Engineering 4 (2), 2128-2137. https://doi.org/10.1016/j.jece.2016.03.030

Rzedowski J. (1983). Bosque de coníferas. In: Vegetación de México. Editorial Limusa, Ciudad de México, 432 pp.

SEMARNAT. (2018). Anuario estadístico de la producción forestal. Secretaría de Medio Ambiente y Recursos Naturales, Ciudad de México, 298 pp.

Sirén H. and El Fellah S. (2017). Androgens, oestrogens, and progesterone concentrations in wastewater purification processes measured with capillary electrophoresis. Environmental Science and Pollution Research 24, 16765-16785. https://doi.org/10.1007/s11356-017-9060-z

Smol M. (2023). Circular economy in wastewater treatment plant-water. Energy and Raw Materials Recovery. Energies 16 (9). https://doi.org/10.3390/en16093911

Sophia C. and Lima E. (2018). Removal of emerging contaminants from the environment by adsorption. Ecotoxicology and Environmental Safety 150, 1-17. https://doi.org/10.1016/j.ecoenv.2017.12.026

Thommes M., Kaneko K., Neimark A., Olivier J., Rodriguez-Reinoso F., Rouquerol J. and Sing K. (2015). Physisorption of gases, with special reference to the evaluation of surface area and pore size distribution (IUPAC technical report). Pure and Applied Chemistry 87 (9-10), 1051-1069. https://doi.org/10.1515/pac-2014-1117

Üner O. and Bayrak Y. (2018). The effect of carbonization temperature, carbonization time and impregnation ratio on the properties of activated carbon produced from *Arundo donax*. Microporous and Mesoporous Materials 268, 225-234. https://doi.org/10.1016/j.micromeso.2018.04.037

Valles-Gándara A.G. and Valadez-Castro R.C. (2006). Evaluación de índices de competencia independientes de la distancia para predecir el crecimiento de bosques mezclados en San Dimas, Durango. Revista Chapingo Serie Ciencias Forestales y del Ambiente 12 (1), 39-44.

Vela-Carrillo A.Z., Martínez R.J., Godínez L.A., Pérez-Bueno J. de J., Espejel-Ayala F. and Robles I. (2024). Study of chemical, kinetic, and theoretical sorption properties of activated carbons obtained from agro-industrial origin: comparison of anionic and cationic model molecules. Biomass Conversion and Biorefinery 14, 733-750. https://doi.org/10.1007/s13399-022-02367-7

Vidal M.V., Rodríguez A., Barrios K.M., Ocampo J. and Lara W.B. (2018). Potencial de residuos agroindustriales para la síntesis de carbón activado: una revisión. Scientia et Technica 23 (3), 411-419.

Zhang J., Nguyen M.N., Li Y., Yang C. and Shäfer A.I. (2020). Steroid hormone micropollutant removal from water with activated carbon fiber-ultrafiltration composite membranes. Journal of Hazardous Materials 391, 1-14. https://doi.org/10.1016/j.jhazmat.2020.122020